Int J Multiphase Flow Vol 18, No 1, pp 51–63, 1992
Printed in Great Britain

0301-9322/92 $5.00 + 0.00

STABILITY IN A TWO-DIMENSIONAL HAGEN–POISEUILLE RESUSPENSION FLOW

K. ZHANG,[1] A. ACRIVOS[1] and U. SCHAFLINGER[2]
[1]The Levich Institute, The City College of CUNY, New York, NY 10031, U.S.A.
[2]Institut fur Strömungslehre und Warmeübertragung, Technische Universitat Wien, Vienna, Austria

(Received 24 August 1990; in revised form 5 August 1991)

Abstract—A linear stability analysis of a viscous resuspension flow, which develops from an initially well-mixed suspension flowing along a two-dimensional channel, is described. The analysis is based on a two-fluid model in which the non-uniformity of the particle concentration distribution within the suspended layer is ignored. Numerical solutions to the relevant Orr-Sommerfeld equations for both temporal and spatial disturbance modes are obtained for the special case of a suspension of spherical particles in water and flowing in a duct with vertical spacing 0.02 m. It is found that the resuspension flow is convectively unstable and that the largest amplification occurs in the range of moderate stability Reynolds numbers. It is also shown that a reduction in the particle concentration in the feed suspension and/or an increase in the relative density ratio of the solid particles to that of the suspending fluid will enhance the instability of the interfacial mode.

Key Words. resuspension flow, stability, interfacial mode

1. INTRODUCTION

A few years ago, Gadala-Maria (1979) inferred from some viscometric experiments that an initially settled bed of negatively buoyant particles in contact with a clear fluid above it could be resuspended when subjected to shear even under conditions of small Reynolds numbers. This phenomenon of "viscous resuspension" was subsequently verified by direct observations and was then investigated for a handful of fully-developed, unidirectional flows (Leighton & Acrivos 1986; Schaflinger *et al.* 1990). Appropriate experiments (Schaflinger *et al.* 1990) have shown, however, that under certain circumstances the interface between the resuspended layer and the clear fluid above becomes unstable to interfacial waves, which are amplified as they travel downstream in a way similar to those observed in gravity settlers beneath inclined walls (Herbolzheimer 1983; Shaqfeh & Acrivos 1987; Borhan & Acrivos 1988; Borhan 1989). Thus, the determination of the stability characteristics of these laminar base flows is a matter of obvious interest especially since, in this case, such instabilities should lead to a greater degree of resuspension than if the flow remained laminar and steady.

In this paper, we shall examine, on the basis of a linear analysis, the stability of the resuspended layer within a plane Hagen–Poiseuille flow, which is fully developed from an initially well-mixed suspension having a particle volume concentration ϕ_s and flowing along a two-dimensional duct, as shown schematically in figure 1. This laminar base flow was studied in our previous publication

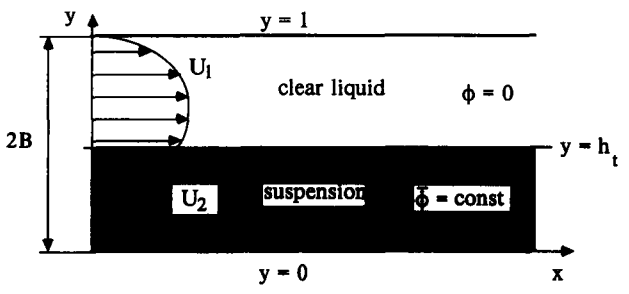

Figure 1. Flow configuration for a two-dimensional Hagen–Poiseuille flow with a resuspended layer

(Schaflinger *et al.* 1990), where it was shown that the extent of the resuspension was governed by a modified Shields number,

$$\kappa = \frac{9}{16}\frac{\mu_1 Q}{B^3 g(\rho_2 - \rho_1)}, \qquad [1]$$

which provides a measure of the ratio of viscous forces to those of gravity. Here $2B$ refers to the vertical spacing of the duct, Q is the volume flux of the suspending fluid per unit depth, μ_1 and ρ_1 denote, respectively, the viscosity and the density of the suspending fluid, ρ_2 is the density of the suspended solid particles and g is the gravitational constant. It turns out that the dimensionless height h, and the particle concentration profile $\phi(y)$ of the resuspended layer, as well as the velocity profiles within both the clear fluid and the suspension, are uniquely determined via the solution of the mass and momentum conservation equations if the two basic parameters ϕ_s and κ are given and the suspension is modelled as a Newtonian fluid whose effective properties depend on the concentration in a known way. The particle concentration profile ϕ within the flowing suspension will of course be non-uniform across the duct and will become uniform only in the limiting case of large Shields numbers.

In principle, it should be possible of course to formulate the stability problem in terms of an Orr-Sommerfeld equation which would include terms arising from the continuous variation of ϕ with position. However, due to the rapid change of ϕ in the vicinity of the interface beneath the clear fluid, as shown in figure 2, and to the presence of its derivatives up to third order in the corresponding Orr-Sommerfeld equation, any attempt to solve the latter is bound to encounter numerical difficulties such as very slow convergence and large CPU times. But, in view of the fact that, in general, the particle concentration is almost uniform within the flowing suspension except within a thin transition layer underneath the suspension–clear fluid interface, it appears reasonable to perform the stability analysis by modeling the suspension as a Newtonian fluid with position-independent physical properties. Thus, the base state is taken to consist of a stratified shear flow of two superposed fluids of different viscosity and density with parabolic velocity profiles, which satisfy the requirement that the velocity and the shear stress be continuous at the interface.

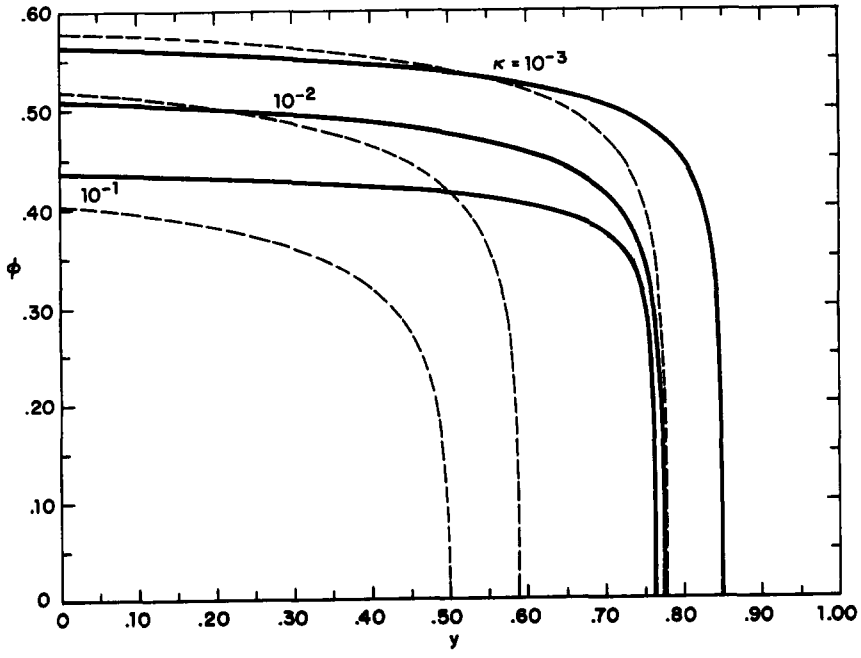

Figure 2. Particle concentration profiles for $\phi_s = 0.1$ (dashed curves), $\phi_s = 0.3$ (solid curve) and $\kappa = 10^{-3}$, 10^{-2}, 10^{-1}.

Moreover, in view of the analysis presented earlier (Schaflinger *et al.* 1990), the height h_t of the resuspended layer and the mean particle concentration,

$$\bar{\phi} \equiv \frac{1}{h_t}\int_0^{h_t} \phi(y)\,\mathrm{d}y,$$

can be taken as known functions of the two independent parameters of the base state, viz. κ and ϕ_s.

The linear, temporal stability of two superposed fluids in a channel flow was studied by Yih (1967), Yiantsios & Higgins (1988) and several other authors (Kao & Park 1972; Hooper & Boyd 1983, 1987; Hinch 1984). Yih (1967) considered long-wavelength disturbances and demonstrated that viscosity stratification alone can give rise to an interfacial mode which is unstable even for vanishingly small Reynolds numbers (Re). Yiantsios & Higgins (1988) extended Yih's work and investigated the effects on the interfacial mode of several geometric and physical parameters, such as the thickness ratio, the viscosity ratio and the density ratio of the two fluids, as well as the surface tension, each of which was allowed to vary independently. In addition, they reported that, at sufficiently large Re, the flow may also be unstable to a shear mode, which is essentially a disturbance of the Tollmien–Schlichting type modified by the presence of an interface.

We shall study both the temporal and the spatial stability of this flow by solving the eigenvalue problem for the Orr-Sommerfeld equations subjected to appropriate boundary conditions at the walls and matching conditions at the interface. This is accomplished numerically using the well-known shooting method with ortho-normalization (Shaqfeh & Acrivos 1987). We find that, whereas the shear mode, similar to that noted by Yiantsios & Higgins (1988), is unstable at large stability Re values of order 10^4 (the Re to be defined later is based on Q and on the properties of the suspending fluid), the interfacial mode is unstable at small and moderate Re, a parameter range of practical interest in the study of the viscous resuspension. Thus, we shall focus on the instabilities due to this interfacial mode. Also, we shall restrict our analysis to cases for which the whole sediment has resuspended, because a sediment layer at the bottom of the duct will exist only when Q is small, in which the flow would be expected to be less unstable.

We shall also study the nature of this instability, i.e. whether it is convective or absolute [see Bers (1983) for a rigorous discussion of absolute and convective instabilies], and shall show that, for the case of a suspension of spherical particles in water and flowing in a duct with vertical spacing 0.02 m, this is always convective—thereby implying that unstable interfacial disturbances will grow spatially in the resuspension flow. Moreover, we shall find that Gaster's relation (Drazin & Reid 1967) between the temporal and the spatial modes applies with good accuracy within the parameter range covered by our calculations, and that therefore both the temporal and spatial analyses are equally capable of describing the spatial development of interfacial waves.

In the next section we shall state the mathematical problem for the linear stability analysis and describe our numerical procedure. The numerical results will then be presented in section 3, and, finally, in section 4, the applicability of our stability calculations (which were based on a simplified model of the base state) to physically relevant resuspension flows will be discussed.

2. THE LINEAR STABILITY ANALYSIS

2.1. Mathematical formulation

The base flow consists of two parabolic velocity profiles U non-dimensionalized by $Q/2B$:

$$U_1 = K[\mathrm{C}(y-1) - \tfrac{1}{2}(y^2-1)] \qquad [2a]$$

and

$$U_2 = K\left[\frac{1}{\mu}\left(\mathrm{C}y - \frac{y^2}{2}\right)\right], \qquad [2b]$$

where

$$\mathrm{C} = \frac{1}{2}\frac{1+\left(\frac{1}{\mu}-1\right)h_t^2}{1+\left(\frac{1}{\mu}-1\right)h_t}, \qquad [3]$$

and

$$K=\left\{\frac{1}{3}-C\left[\frac{1}{2}+h_t\left(\frac{h_t}{2}-1\right)\right]+\frac{h_t}{2}\left(\frac{h_t^2}{3}-1\right)+\frac{(1-\bar{\phi})h_t^2}{2\mu}\left(C-\frac{h_t}{3}\right)\right\}^{-1}. \quad [4]$$

Here y is the vertical coordinate non-dimensionalized by the total spacing $2B$, and μ is the ratio of the effective viscosity of the suspension to that of the clear fluid. This effective relative viscosity will be represented by means of the empirical relation (Leighton & Acrivos 1986)

$$\mu=\left(1+\frac{1.5\bar{\phi}}{1-\dfrac{\bar{\phi}}{\phi_0}}\right)^2, \quad [5]$$

where ϕ_0 is the maximum particle concentration of a settled bed assumed to equal 0.58 in our calculations. In addition, C denotes a constant which is obtained from the matching conditions at the interface, and K refers to a dimensionless pressure drop coefficient, subscripts 1 and 2 distinguish between the clear fluid and the suspension, respectively.

Since a detailed derivation of the governing equations for the linear stability analysis has already been given by Yih (1967), we shall present, in what follows, only some of the key steps. Thus, if we consider two-dimensional disturbances, we let Φ and Ψ be the perturbation stream functions within the clear fluid and the suspension, respectively, which automatically satisfy the continuity equations. The velocity components become, therefore:

$$u_1=U_1+\Phi_{,y}, \quad v_1=-\Phi_{,x}; \quad [6a]$$

and

$$u_2=U_2+\Psi_{,y}, \quad v_2=-\Psi_{,x}. \quad [6b]$$

The linearized equations and the appropriate boundary conditions for the disturbed flow are then expanded in the usual manner in terms of normal modes with an exponential time factor. Specifically, we have for the perturbation stream functions

$$\Phi(x,y,t)=\varphi(y)\exp[i(\alpha x-\omega t)] \quad [7a]$$

and

$$\Psi(x,y,t)=\psi(y)\exp[i(\alpha x-\omega t)], \quad [7b]$$

where $\varphi(y)$ and $\psi(y)$ are the amplitudes of the disturbances and t is the time rendered dimensionless with $4B^2/Q$. In order to determine whether the flow is absolutely or convectively unstable, we shall take both the frequency ω and the wavenumber α to be complex quantities, i.e. we let

$$\omega=\omega_r+i\omega_i \quad \text{and} \quad \alpha=\alpha_r+i\alpha_i.$$

Then, for a temporal analysis, we take the wavenumber α as real, while for a spatial analysis, we prescribe a real frequency ω. In view of [7a, b], we then obtain from the equations of motion the well-known Orr-Sommerfeld equations for the clear fluid,

$$(\alpha U_1-\omega)(\varphi''-\alpha^2\varphi)-\alpha U_1''\varphi=-\frac{i}{\mathrm{Re}}(\varphi''''-2\alpha^2\varphi''+\alpha^4\varphi), \quad [8]$$

and for the suspension,

$$(\alpha U_2-\omega)(\psi''-\alpha^2\psi)-\alpha U_2''\psi=-i\frac{\mu}{\mathrm{Re}(1+\bar{\phi}\epsilon)}(\psi''''-2\alpha^2\psi''+\alpha^4\psi), \quad [9]$$

respectively, in which primes indicate differentiation with respect to y. Moreover, on account of the boundary conditions of no slip and no penetration at the walls, as well as the requirement that the velocity and, in the absence of surface tension, the stresses be continuous at the interface, we obtain in the linear approximation that

$$\varphi=\varphi'=0 \qquad \text{at } y=1, \quad [10a]$$

$$\psi=\psi'=0 \qquad \text{at } y=0, \quad [10b]$$

$$\varphi - \psi = 0 \qquad \text{at } y = h_t, \qquad [10c]$$

$$\varphi' - \psi' = \alpha(U_1' - U_2')\frac{\varphi}{\alpha U_1 - \omega} \qquad \text{at } y = h_t, \qquad [10d]$$

$$\varphi'' - \mu\psi'' = \alpha^2\varphi(\mu - 1) \qquad \text{at } y = h_t \qquad [10e]$$

and

$$i\frac{9\alpha^2\bar{\phi}}{2\kappa}\frac{\varphi}{\alpha U_1 - \omega} = \varphi''' - 3\alpha^2\varphi' - \mu(\psi''' - 3\alpha^2\psi') + i\,\mathrm{Re}\{(\alpha U_1 - \omega)[(1 + \bar{\phi}\epsilon)\psi' - \varphi'] - \alpha[(1 + \bar{\phi}\epsilon)U_2'\psi - U_1'\varphi]\} \qquad \text{at } y = h_t. \qquad [10f]$$

Here $\mathrm{Re} = Q\rho_1/\mu_1$ is the stability Reynolds number which is related to the Shields number κ by

$$\mathrm{Re} = \tfrac{2}{9}\kappa\epsilon\,\mathrm{Ga}, \qquad [11]$$

with the Galileo number $\mathrm{Ga} \equiv 8B^3g\rho_1^2/\mu_1^2$ being constant if the spacing of the duct and the physical properties of the suspending fluid are given. In addition, $\epsilon = (\rho_2 - \rho_1)/\rho_1$ denotes the relative density ratio of the particles to the suspending fluid. We note that, in the stability analysis, the gravitational constant appears only on the l.h.s. of [10f], where it is incorporated in the base state parameter κ.

Equations [8]–[10] constitute an eigenvalue problem for the complex frequency ω or for the complex wavenumber α, respectively. Note that the parameters h_t and $\bar{\phi}$ are taken from the base flow analysis as being known functions of the independent variables ϕ_s and κ and that the new independent parameters introduced by the stability formulation are Re (or Ga) and ϵ.

2.2. Numerical procedure

Several numerical methods have already been developed for solving the Orr-Sommerfeld problem, among which are the well-known shooting method with an ortho-normalization procedure and the compound matrix method (Drazin & Reid 1967). At first, as a cross-check, the eigenvalues of our problem were calculated using both these methods and the results were found to be in good agreement. But since the former turned out to have a larger convergence radius, it was employed almost exclusively for most of the calculations.

The essence of the shooting method with ortho-normalization, which has already been described in detail in an earlier publication (Shaqfeh & Acrivos 1987), is briefed as follows for the case of the temporal analysis. We first define the vector functions

$$\boldsymbol{\varphi} = (\varphi, \varphi', \varphi'', \varphi'''), \quad \boldsymbol{\psi} = (\psi, \psi', \psi'', \psi''') \qquad [12]$$

and express each one of them as linear combination of two solutions which satisfy the boundary conditions at $y = 1$ and $y = 0$, respectively, i.e. we let

$$\boldsymbol{\varphi} = \mathrm{C}_1\boldsymbol{\varphi}_1 + \mathrm{C}_2\boldsymbol{\varphi}_2, \quad \boldsymbol{\psi} = \bar{\mathrm{C}}_1\boldsymbol{\psi}_1 + \bar{\mathrm{C}}_2\boldsymbol{\psi}_2, \qquad [13]$$

and

$$\boldsymbol{\varphi}_1 = (0, 0, 1, 0), \quad \boldsymbol{\varphi}_2 = (0, 0, 0, 1) \quad \text{at } y = 1 \qquad [14]$$

and

$$\boldsymbol{\psi}_1 = (0, 0, 0, 1), \quad \boldsymbol{\psi}_2 = (0, 0, 1, 0) \quad \text{at } y = 0. \qquad [15]$$

Then, for a given set of parameters α, ϕ_s, κ, ϵ and Re and an initial guess for the eigenvalue ω, we integrate [8] and [9] by means of a standard fourth-order Runge–Kutta algorithm, using [14] and [15] as initial conditions, respectively, up to the interface $y = h_t$. Each integration interval $(1, h_t)$ or $(0, h_t)$ was divided into 100 sub-intervals, and the integration was performed within each one of them until a solution accurate to eight-digits was obtained through mesh refinement. Then, the two solutions $\boldsymbol{\varphi}_1$, $\boldsymbol{\varphi}_2$ and $\boldsymbol{\psi}_1$, $\boldsymbol{\psi}_2$, respectively, were verified to be linearly independent using a

method introduced by Conte (1966) and, if necessary, two new linearly independent solutions were generated by the Gramm–Schmidt ortho-normalization procedure. At that point, the integration was allowed to proceed using the new solutions as starting conditions.

At the interface $y = h_t$ the matching conditions yield a set of homogeneous linear, algebraic equations whose complex determinant gives the dispersion relation

$$D(\alpha, \omega) = \begin{vmatrix} \varphi_1 & \varphi_2 & -\psi_1 & -\psi_2 \\ \varphi_1' + A_1\varphi_1 & \varphi_2' + A_1\varphi_2 & -\psi_1' & -\psi_2' \\ \varphi_1'' + A_2\varphi_1 & \varphi_2'' + A_2\varphi_2 & -\mu\psi_1'' & -\mu\psi_2'' \\ \varphi_1''' - A_4\varphi_1' + A_3\varphi_1 & \varphi_2''' - A_4\varphi_2' + A_3\varphi_2 & -\mu\psi_1''' + A_5\psi_1' & -\mu\psi_2''' + A_5\psi_2' \end{vmatrix} \quad [16]$$

with

$$A_1 = \frac{\alpha(U_2' - U_1')}{\alpha U_1 - \omega}, \quad [17a]$$

$$A_2 = \alpha^2(1 - \mu), \quad [17b]$$

$$A_3 = i\alpha \operatorname{Re}\left[U_1' - (1 + \bar{\phi}\epsilon)U_2' - \frac{9\alpha\bar{\phi}}{2\kappa \operatorname{Re}(\alpha U_1 - \omega)} \right], \quad [17c]$$

$$A_4 = 3\alpha^2 + i \operatorname{Re}(\alpha U_1 - \omega) \quad [17d]$$

and

$$A_5 = i \operatorname{Re}(1 + \bar{\phi}\epsilon)(\alpha U_1 - \omega) + 3\mu\alpha^2. \quad [17e]$$

Therefore, the problem reduces to that of finding numerically a complex eigenvalue ω by requiring that

$$D(\omega) = 0.$$

Of course, since our initial guess for ω will not satisfy this requirement, we obtain

$$D(\omega) = D_1.$$

But, because $D(\omega)$ is an analytic function of ω in the neighborhood of the actual eigenvalue (Mack 1976), we are able to generate a new and better guess for ω by means of the recursion formula

$$\omega_{k+1} = \omega_k - \frac{\omega_k - \omega_{k-1}}{D_k - D_{k-1}} D_k. \quad [18]$$

But, in order to make use of [18], we need to repeat the entire integration procedure for a slightly different guess, $\omega_2 = \omega_1 + \varepsilon$, with ε being an arbitrary small complex number to obtain

$$D(\omega_2) = D_2.$$

Then [18] is applied until the following convergence criteria are satisfied:

$$|D_k - D_{k-1}| \leqslant 10^{-10}; \quad \frac{|\omega_k - \omega_{k-1}|}{|\omega_k|} \leqslant 10^{-8}; \quad \frac{|D_k - D_{k-1}|}{|D_1|} \leqslant 10^{-8}. \quad [19]$$

In addition, in order to enhance the rate of convergence, a parameter continuation in α (or sometimes in other parameters, such as h_t or $\bar{\phi}$) is employed, by selecting the actual eigenvalue ω at a certain wavenumber α as the initial guess for the eigenvalue at the wavenumber $\alpha + \Delta\alpha$, where $\Delta\alpha$ is a small increment in the wavenumber α. In this way, the convergence criteria [19] could be met in most cases after 6–8 iterations.

3. NUMERICAL RESULTS

In this section we shall present and discuss our numerical results which were obtained with the Galileo number in [11] kept constant at 7.9×10^7, corresponding to water at 20°C and to a duct spacing $2B = 0.02$ m. The other parameters ϕ_s, ϵ and κ (or Re) were set at varous values of practical interest and, in particular, Re was allowed to vary up to $O(10^3)$. Within this range of Re, the instabilities are due to the interfacial mode, which was traced by means of parameter continuation,

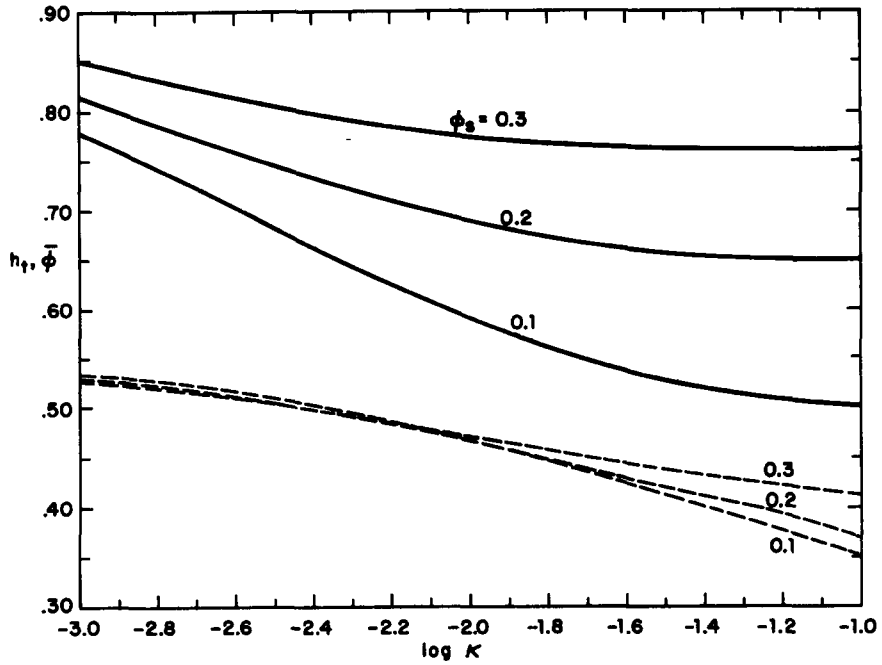

Figure 3. Height h_f (solid curves) and mean particle concentration $\bar{\phi}$ (dashed curves) of the suspension vs log(κ) for $\phi_s = 0.1, 0.2, 0.3$.

starting with a pair of values for the frequency and the wavenumber given in a previous publication (Yiantsios & Higgins 1988).

To begin with, we depict in figure 3 the variation of h_f and $\bar{\phi}$, obtained from the base state analysis (Schaflinger *et al.* 1990), as functions of the modified Shields number κ for $\phi_s = 0.1, 0.2, 0.3$. It is seen that, with increasing of κ, both h_f and $\bar{\phi}$ (and, hence, the viscosity ratio μ) are reduced, as required by particle mass conservation in the base state flow. We note here that, due to the dependence of μ on $\bar{\phi}$, given by [5], the difference in μ for the different values of ϕ_s shown in figure 3 is considerable, even though the variation of $\bar{\phi}$ with ϕ_s is not that great.

We first tried to establish whether the flow was absolutely or convectively unstable. This was done by examining the location, in the complex ω-plane, of the double roots (α_0, ω_0) of the dispersion relation [16] which satisfy simultaneously $D(\alpha, \omega) = 0$ and $\partial D/\partial\alpha = 0$ (Triantafyllou & Dimas 1989). Then the flow instability is of the absolute type if one such double root can be found which is located in the upper-half ω-plane and which is formed from the coalescence of two roots of the dispersion relation [16] corresponding to one left- and one right-traveling wave. But since, within the parameter range covered by our calculations, all of the double roots which we found were located (as illustrated in figure 4 for a typical case) well below the real axis $\omega_i = 0$, we conclude that the instability, if it exists, will always be convective for the particular system under consideration.

It is known (Bers 1983) that the existence of a convective instability implies a spatially developing response to a steady harmonic excitation. Specifically, for the present resuspension flow, it implies that unstable interfacial waves will grow in space. In order to find the properties of such waves, we performed both a spatial and a temporal analysis and compared their predictions by converting the temporal amplification rate ω_i into the spatial amplification rate $-\alpha_i$ using Gaster's relation (Drazin & Reid 1967, p. 352):

$$-\alpha_i = \frac{\omega_i}{c_g}, \qquad [20]$$

where $c_g = \partial\omega_r/\partial\alpha$ denotes the group wave velocity. This relation has been proved valid if the amplification rates of the disturbances are small. Typical comparisons are shown in figure 5 in the form of spatial amplification rates for $\epsilon = 0.1$, Re = 1560 and $\phi_s = 0.1, 0.2, 0.3$, respectively, where the dashed curves represent the predicted spatial amplification rates converted from the results of

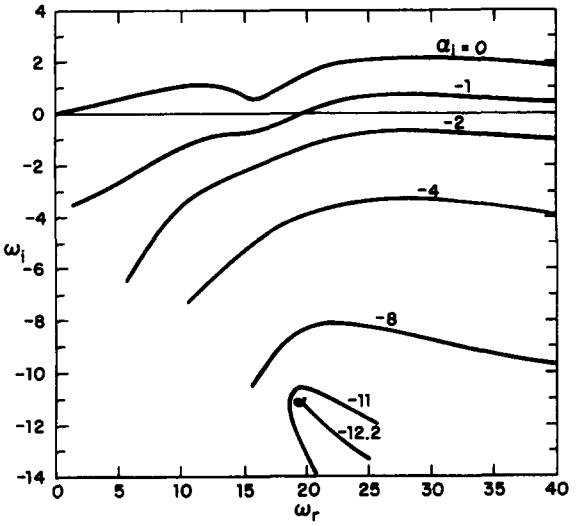

Figure 4. Instability curves for $\phi_s = 0.1$, $\epsilon = 0.1$, Re = 1560 and for a variety of α_i

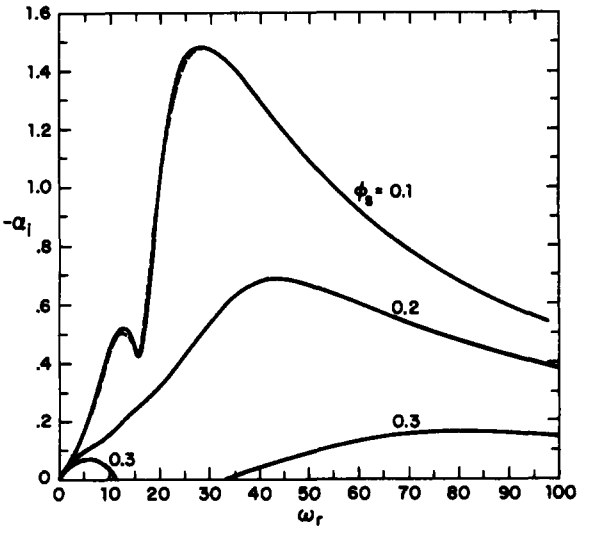

Figure 5. Spatial amplification rate $-\alpha_i$ for $\phi_s = 0.1$, 0.2, 0.3, $\epsilon = 0.1$ and Re = 1560. The solid lines are results from the spatial analysis; the dashed lines are from the temporal analysis together with [20].

the temporal analysis, and the solid curves are from the spatial analysis. We see that the two sets of curves almost coincide. In fact, the agreement is even better when ϵ and/or Re are smaller, because the corresponding amplification rates are smaller. Thus, we conclude that both the temporal and spatial analyses are equally capable of describing the spatial development of interfacial growing waves in this particular resuspension flow, and hence, in what follows, we shall present our numerical results only in terms of the temporal mode.

Figure 6 depicts the topology of the neutral stability curves in the Re–α_r plane for $\phi_s = 0.1$, 0.2, 0.3 and $\epsilon = 0.01$ (solid curves), and for $\phi_s = 0.2$ and $\epsilon = 0.001$, 0.1 (broken curves). The arrow to the left of some of the curves indicates that a further decrease in Re will lead to the formation of a sediment layer at the bottom of the duct. We see that the resuspension flow is, in general, unstable and that, in the case of a small feed concentration ϕ_s and/or of a large density ratio ϵ, instabilities arise even when a sediment still exists at the bottom of the duct. We also see that each neutral curve consists of one lower and one upper branch (for $\phi_s = 0.3$, the upper branch is located in the

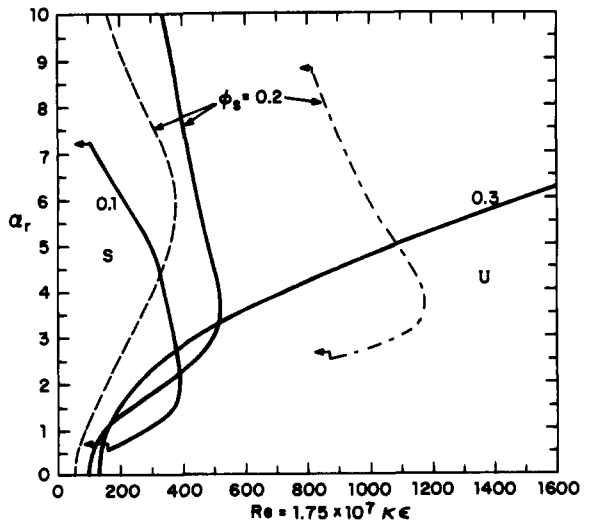

Figure 6. Neutral stability diagram for $\phi_s = 0.1$, 0.2, 0.3 and $\epsilon = 10^{-2}$ (solid curves); and $\phi_s = 0.2$ and $\epsilon = 10^{-3}$ (curve — — —), 0.1 (curve — · —). Stable regions are denoted by S, unstable regions by U. Arrows represent the values of Re below which a sediment layer forms in the base state

region of large wavenumber and is not shown in the figure), and that the turning point occurs at an Re value which increases with an increase in the parameters ϕ_s and ϵ. Therefore, the wavelengths of the unstable disturbances are within two distinct ranges, long and short respectively, and, with increasing Re, interfacial disturbances over the whole spectrum of wavelengths will finally become unstable.

The instability characteristics of these interfacial disturbances for a wide range of wavelengths are illustrated in figures 7–9, where the real and imaginary parts, respectively, of the frequency ω have been plotted vs the real wavenumber α_r for a relative density ratio $\epsilon = 0.01$, and for a variety of values of the feed concentration ϕ_s and of Re. It is of some interest to note that, as seen in figures 7(a), 8(a) and 9(a), the frequency ω_r is almost linear in the wavenumber α_r except when the wavenumbers of the disturbances are small. On the other hand, we see in figures 7(b), 8(b) and 9(b) that each curve of the amplification rate ω_i vs α_r has, in general, two peaks; and that the corresponding magnitudes of ω_i at these peaks vary in a somewhat complicated way with the parameters ϕ_s and Re. Specifically, when the feed suspension is dilute, e.g. in the case of $\phi_s = 0.1$, the unstable modes at the first peaks have relatively low growth rates and that the fastest growing disturbances are those at the second peaks with the wavelengths approx. 0.6 times the spacing of the duct. However, the amplification rates at the first peaks become more substantial as the feed concentration increases. In fact, when $\phi_s = 0.3$, the largest amplification occurs at the first peak until Re is sufficiently large that the amplification rates at the second peaks again overtake those of the first. It should be noted that, since the wavelengths of the unstable modes at the second peaks are now approximately one-fifth the spacing of the duct, there is some question as to whether their dominant role is spurious—in that it could be due to the simplifications introduced in the base flow velocity and concentration profiles prior to performing the stability analysis. We shall discuss this aspect in detail in the next section.

We also see from figures 7(b), 8(b) and 9(b) that, for given ϵ and Re, the maximum amplification rate, which we shall denote as $(\omega_i)_{max}$, decreases considerably (note the different scalings in these figures) as the feed concentration ϕ_s is increased. This implies that a reduction in the particle concentration of the feed suspension will enhance the degree of instability in the resuspension flow. This enhancement is mainly due to the fact that, as shown in figure 3, the height, h_f, of the resuspended layer in the duct decreases dramatically with a decrease in ϕ_s as required by particle mass conservation in the base flow. Recall that the asymptotic analysis for short-wave instabilities in the stratified flow of two immiscible fluids (Yiantsios & Higgins, 1988) showed that, in the absence of gravitational and surface tension effects, the amplification rate ω_i is proportional to the square of the shear rate at the interface. Such a proportionality was also given by Hinch (1984) who provided a simple physical explanation for the instability mechanism at the interface. Because

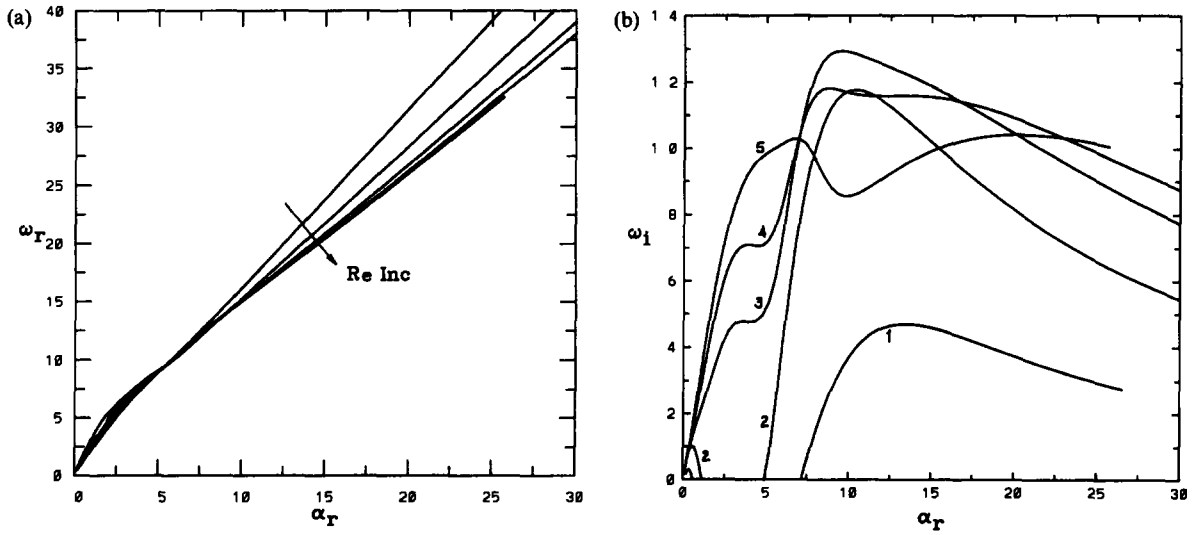

Figure 7. The real (a) and imaginary (b) parts of the frequency ω vs α_r for $\phi_s = 0.1$, $\epsilon = 0.01$ and various values of Re: (1) 160; (2) 320; (3) 550; (4) 730; (5) 1050.

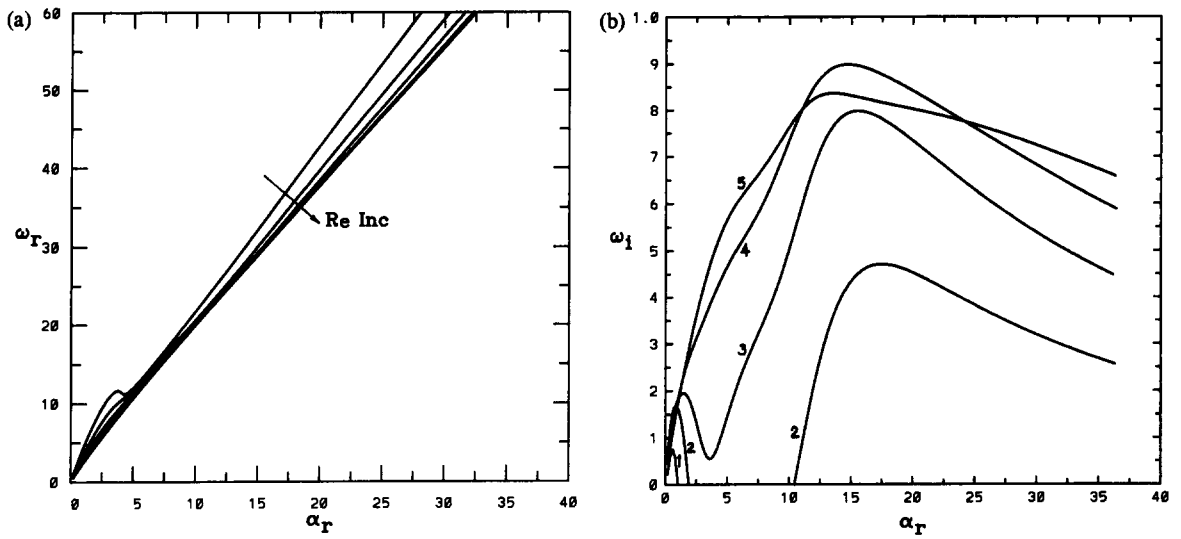

Figure 8 The real (a) and imaginary (b) parts of the frequency ω vs α_r for $\phi_s = 0.2$, $\epsilon = 0.01$ and various values of Re: (1) 160; (2) 320; (3) 550; (4) 900; (5) 1420.

the shear rate at the interface is a monotonically decreasing function of h_f, as can be easily verified from [2]–[4], the reduction in the feed concentration ϕ_s leads to the pronounced increase in the shear rate and, hence, in $(\omega_i)_{max}$.

In addition, as remarked by Schaflinger *et al.* (1990), the height h_f of the resuspended layer is restricted by the existence of a plane of vanishing shear stress, which, in the limit of infinite κ, coincides with the interface between the resuspended layer and the clear fluid above it. This limiting case has important implications as regards the stability of this system because the interfacial mode is neutrally stable when the slope of the base velocity profile vanishes at the interface (Yiantsios & Higgins 1988). Consequently, all interfacial disturbances will trend towards a neutrally stable state in the limit of infinite κ or Re. This trend can be seen in figures 7(b), 8(b) and 9(b) and is more clearly illustrated in figure 10, where the maximum amplification rate $(\omega_i)_{max}$ is shown for $\phi_s = 0.2$ and for $\epsilon = 10^{-3}, 10^{-2}, 10^{-1}$. We see that, when $\epsilon = 10^{-3}$, this maximum amplification rate approaches zero as Re limits approx. 3000, where it can be ascertained that the shear rate at the interface h_f is becoming vanishingly small. For larger ϵ, the same trend can be observed but at much larger Re. We also see that, with increasing Re, $(\omega_i)_{max}$ first increases sharply until it reaches a peak value and then decreases gradually, thereby indicating that the disturbances restabilize. This

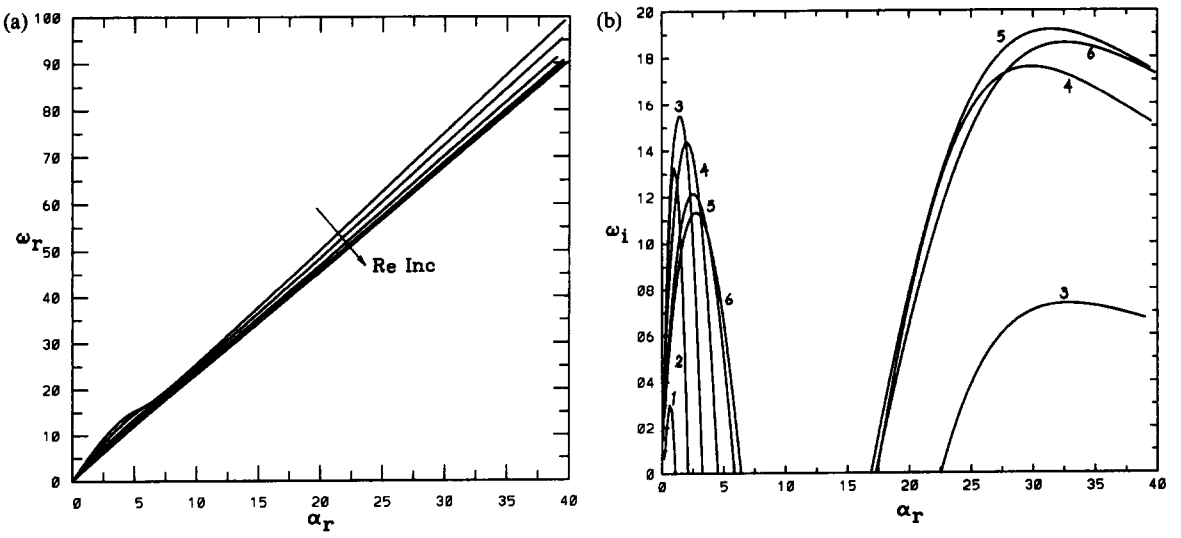

Figure 9. The real (a) and imaginary (b) parts of the frequency ω vs α_r for $\phi_s = 0.3$, $\epsilon = 0.01$ and various values of Re: (1) 160, (2) 270; (3) 500; (4) 900; (5) 1420; (6) 1660

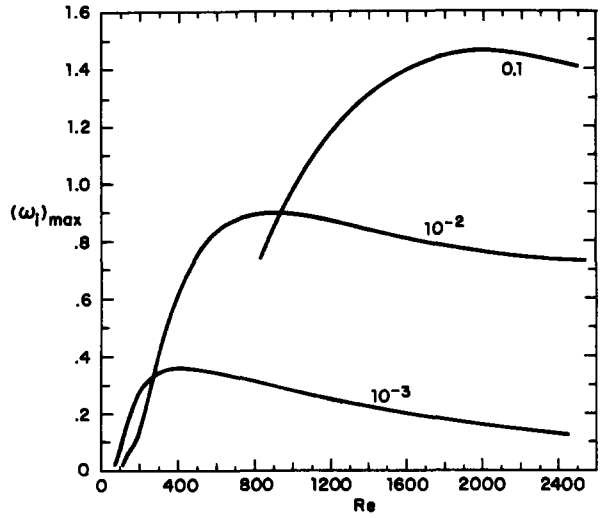

Figure 10. The maximum amplification rate $(\omega_i)_{max}$ for $\phi_s = 0.2$ and $\epsilon = 10^{-3}, 10^{-2}, 10^{-1}$.

prediction regarding the restabilization of the interfacial mode was also reported previously by Shaqfeh & Acrivos (1987) for the convective flow which arises in inclined particle settlers. Nevertheless, it should be emphasized that this does not imply the existence of an experimentally observable restabilization of unstable interfacial waves in such flows because, on account of three-dimensional disturbances, an increase in Re does not restabilize the flow, but rather changes the direction of the growing modes and, more specifically, that of the most rapidly amplified mode, which in general is oblique (Magen & Patera 1986). Also, on account of the fact that this restabilization is predicted to occur in the range of large Re, it is natural to expect that the shear mode of the Tollmien–Schlichting type may become unstable and dominate the instability.

We also see from figure 10, that the peak value of $(\omega_i)_{max}$ increases with an increase in the relative density ratio ϵ. The reason for this is somewhat subtle. Again referring to figure 10, we note that, for increasing ϵ, the maximum amplification $(\omega_i)_{max}$ attains its peak value at larger Re but, on the other hand, in view of [11], at smaller κ. An increase in Re obviously entails a larger inertial effect on the instability of the interfacial mode, whereas on account of the fact that $\bar{\phi}$ and, hence, μ are monotonically decreasing functions of κ, a decrease in κ enhances the viscosity stratification at the interface and therefore the driving force for the instability. Thus, the combination of these two effects, which follow from an increase in ϵ, leads to an enhanced degree of instability in spite of the stronger stabilization introduced by the greater density stratification.

4. SUMMARY AND DISCUSSION

The results of a linear stability analysis were presented dealing with the formation of interfacial waves in a two-dimensional Hagen–Poiseuille resuspension flow. The non-uniformity of the particle concentration within the suspension was ignored, so that the base system consisted of a stratified shear flow of two superposed fluids with different but position-independent physical properties. The spacing and the mean particle concentration of the suspension were calculated from the solution of the laminar resuspension flow problem described previously (Schaflinger *et al.* 1990).

Numerical solutions of the resulting Orr-Sommerfeld system of equations, for the special case of a suspension of spherical particles in water and flowing in a duct with vertical spacing 0.02 m, were obtained by means of a classical shooting method with ortho-normalization. The computations focused primarily on the instabilities due to the interfacial mode. It is found that the resuspension flow is always convectively unstable for this case† and that the amplification rate of the interfacial disturbances first increases sharply with increasing stability Re until it reaches a peak value beyond which it begins to decrease gradually. It is also shown that a reduction in the particle

†This, of course, does not exclude the possible existence of an absolute instability for a different range of parameters.

concentration of the feed suspension and/or an increase in the relative ratio of density of the solid particles to that of the suspending fluid will enhance the degree of instability in such a flow.

The principal assumption made in this work, that the particle concentration in the resuspended layer is uniform, restricts the range of disturbance wavelengths for which the present theory is applicable. Specifically, under this assumption, our analysis obviously no longer applies for wavelengths which are shorter than the thickness of the transition layer within which, as shown in figure 2, the actual concentration distribution $\phi(y)$ varies rapidly. In fact, one can expect that the predicted short-wavelength instability could have been eliminated or reduced if the continuous variation with position of the actual concentration profile in the real resuspension flow could somehow have been taken into account. In the case of shearing flows of two homogeneous fluids, it has been shown (Hinch 1984; Yiantsios & Higgins 1988) that the instability of short-wavelength disturbances may always be stabilized either by surface tension or by diffusion, depending on whether the two fluids are immiscible or miscible. The stabilizing effect of diffusion on short-wave instabilities was also demonstrated for the problem of miscible displacements in porous media (Tan & Homsy 1986), where it was found that, whereas the amplification rate of unstable disturbances increases with increasing wavenumber without bound if the diffusion effect is ignored, a cut-off in the instability wavenumber is always encountered whenever this effect is taken into account. In the present problem, where surface tension is absent, the actual particle concentration and, hence, the viscosity beneath the interface are rapidly but *continuously* varying functions of position. Thus, in view of the fact that diffusion smooths concentration profiles, the assumption in our analysis that both these profiles are uniform, which leads to a jump in concentration and viscosity at the interface, is equivalent to ignoring diffusion effects in systems of two miscible, homogeneous fluids. Therefore, we should expect our analysis to overestimate the influence of short-wavelength instabilities.

Nevertheless, we feel that the major, as well as the more practically interesting predictions of our simple model, such as the predicted dependence of the instability on the parameters Re, ϕ_s and ϵ, are sound (at least qualitatively) because these predictions are based essentially on the shearing mechanism (Hinch 1984), which generates the instabilities at the interface, and on the way in which the amplification rate of the unstable disturbances varies with the shear rates and the viscosities on either side of the interface. In addition, as seen in the last section, the wavelengths of the most amplified modes are, in general, large compared to the thickness of the transition layer in the base state concentration profile. Thus, there is reason to believe that the amplification rates of these modes would not be altered substantially if the non-uniformity of the actual particle concentration was taken into account. A possible exception to this may be in the case $\phi_s = 0.3$, where the second peaks of the ω_i curves in figure 9(b) occur at values of the dimensionless wavelength approximately equal to 0.2, which appears to be in a range comparable to the thickness of the transition layer.

Acknowledgements—This research was supported in part by a grant from the U.S. Department of Energy (Grant No. DE-FG02-20ER14139.A000), by the U.S.–Austria Cooperative Program (NSF-INT-9012193), by computing resources provided by the City University of New York Computer Center and by the State of New York under its Einstein Chair Program. The authors are grateful to Professor G. Triantafyllou for sharing with them his expert knowledge of absolute and convective instability.

REFERENCES

BERS, A. 1983 Space–time evolution of plasma instabilities—absolute and convective. In *Handbook of Plasma Physics* (Edited by ROSENBLUTH, M. N. & SAGDEEV, R. Z.). North-Holland, New York.

BORHAN, A. 1989 An experimental study of the stability and efficiency of inclined supersettlers. *Phys. Fluids A* **1**, 108–124.

BORHAN, A. & ACRIVOS, A. 1988 The sedimentation of nondilute suspensions in inclined settlers. *Phys. Fluids* **31**, 3488–3501.

CONTE, S. D. 1966 The numerical solution of linear boundary value problems. *SIAM Rev.* **8**, 309–321.

DRAZIN, P. G. & REID, W. H. 1967 *Hydrodynamic Stability*. Cambridge Univ. Press, Cambs.

GADALA-MARIA, F. A. 1979 The rheology of concentrated suspensions. Ph.D. Dissertation, Stanford Univ., CA.

HERBOLZHEIMER, H. 1983 Stability of the flow during sedimentation in inclined channels. *Phys. Fluids* **26,** 2043–2054.

HINCH, E. J. 1984 A note on the mechanism of the instability at the interface between two shearing fluids. *J. Fluid Mech.* **144,** 463–465.

HOOPER, A. P. & BOYD, W. G. C. 1983 Shear-flow instability at the interface between two viscous fluids. *J. Fluid Mech.* **128,** 507–528.

HOOPER, A. P. & BOYD, W. G. C. 1987 Shear-flow instability due to a wall and a viscosity discontinuity at the interface. *J. Fluid Mech.* **179,** 201–225.

KAO, T. W. & PARK, C. 1972 Experimental investigations of the stability of channel flows. Part 2. Two-layered co-current flow in a rectangular channel. *J. Fluid Mech.* **52,** 401–423.

LEIGHTON, D. & ACRIVOS, A. 1986 Viscous resuspension. *Chem. Engng Sci.* **41,** 1377–1384.

MACK, L. M. 1976 A numerical study of the temporal eigenvalue spectrum of the Blasius boundary layer. *J. Fluid Mech.* **73,** 497–520.

MAGEN, M. & PATERA, A. T. 1986 Three-dimensional linear instability of parallel shear flows. *Phys. Fluids* **29,** 364–367.

SCHAFLINGER, U., ACRIVOS, A. & ZHANG, K. 1990 Viscous resuspension of a sediment within a laminar and stratified flow. *Int. J. Multiphase Flow* **16,** 567–578.

SHAQFEH, E. S. & ACRIVOS, A. 1987 The effects of inertia on the stability of the convective flow in inclined particle settlers. *Phys. Fluids* **30,** 960–973.

TAN, C. T. & HOMSY, G. M. 1986 Stability of miscible displacements in porous media: rectilinear flow. *Phys. Fluids* **29,** 3549–3556.

TRIANTAFYLLOU, G. S. & DIMAS, A. A. 1989 Interaction of two-dimensional separated flows with a free surface at low Froude numbers. *Phys. Fluids A* **1,** 1813–1821.

YIANTSIOS, S. G. & HIGGINS, B. G. 1988 Linear stability of plane Poiseuille flow of two superposed fluids. *Phys. Fluids* **31,** 3225–3238.

YIH, C. S. 1967 Instability due to viscosity stratification. *J. Fluid Mech.* **27,** 337–352.